



建造物における銅及び黄銅製金具周辺に見られた木部の白色化に関する研究：水戸弘道館孔子廟と旧岩崎末廣別邸を対象に

| | |
|----------|--|
| 著者 | 周 怡杉 |
| 雑誌名 | 世界遺産学研究 |
| 巻 | 1 |
| ページ | 68-73 |
| 発行年 | 2016-03-31 |
| その他のタイトル | Research about Whitening Phenomenon of Woods Associated with Copper and Brass Components of Architectures : in the Cases of Confucian Temple of Kodokan of Mito Domain and Old Iwasaki-ke Suehiredo-bettei Villa |
| URL | http://doi.org/10.15068/00137498 |

建造物における銅及び黄銅製金具周辺に見られた木部の白色化に関する研究：水戸弘道館

孔子廟と旧岩崎末廣別邸を対象に

Research about Whitening Phenomenon of Woods Associated with Copper and Brass Components of
Architectures: in the Cases of Confucian Temple of Kodokan of Mito Domain and Old Iwasaki-ke
Suehiro-bettei Villa

周 怡杉

Zhou Yishan

1. Introduction

Wood adjacent to metal can be adversely affected under certain conditions¹, which are generally observed in the case of cultural properties and artifacts. A whitening phenomenon of woods associated with metal components is commonly observed in Japanese historic architecture. Until now, which has not been profoundly studied.

In the Confucian Temple of Kodokan of Mito Domain (水戸弘道館孔子廟, Mito City, Ibaraki Prefecture, reconstructed in 1970s) and Old Iwasaki-ke Suehiro-bettei Villa (旧岩崎家末廣別邸, Tomisato City, Chiba Prefecture, constructed in 1920s-1930s), the whitening phenomenon of wood adjacent to copper and brass components were observed.

To enhance the understanding about this phenomenon, and support more comprehensive conservation activities in the future, investigations were conducted by in-situ and extra-situ investigation methods. The nondestructive in-situ investigations included microscopic observation, elemental investigation and colorimetric measurements, extra-situ analysis included means of FTIR spectroscopy analysis, XRD analysis, SEM-EPMA, and IC analysis.

2. Study for the Confucian Temple of Kodokan of Mito

Domain

The Kodokan of Mito Domain was constructed in 1841, as a school to provide education on Confucianism, history, astronomy, mathematics, music, military strategy, arts, etc., for warriors and their children. The Confucian Temple is one of the vital constituents of the Special Historic Site of Kodokan^{2,3}. The original structures were constructed in a style that imitated the Confucian Temple of China, and were ruined in 1945 by war. Afterwards, reconstruction was conducted on the surviving foundation in 1970. The main structures were made from zelkova wood (ケヤキ). After the 311 East Japan Earthquake, in order to repair the damaged parts and enhance structural stability, a restoration was conducted⁴.

The whitening phenomenon of woods was observed adjacent to metallic components in the Confucian Temple. In addition, in the restoration of 2011, several Nageshi (長押, a horizontal piece of timber to connect pillars) were substituted. Since then, the removed Nageshi were exposed to the rural environment. After experiencing exposure for 3 years, traces of copper components and the whitening phenomenon of adjacent wood were still clearly distinguishable. Therefore, the removed Nageshi became an excellent object for

Table 1 Correlation coefficients (r) for I(Cu) and L* value for vertical window frames

| No. of section | r | No. of section | r | No. of section | r | No. of section | r | No. of section | r | No. of section | r |
|----------------|--------|----------------|--------|----------------|--------|----------------|--------|----------------|--------|----------------|--------|
| 5-WLL | 0.9885 | 6-WLL | 0.8309 | 7-WLL | 0.6901 | 9-WLL | 0.9733 | 10-WLL | 0.7022 | 11-WLL | 0.9545 |
| 5-WUL | 0.9503 | 6-WUL | 0.9449 | 7-WUL | 0.9475 | 9-WUL | 0.9811 | 10-WUL | 0.7415 | 11-WUL | 0.8667 |
| 5-WLR | 0.9582 | 6-WLR | 0.9662 | 7-WLR | 0.5214 | 9-WLR | 0.7731 | 10-WLR | 0.9456 | 11-WLR | 0.9577 |
| 5-WUR | 0.9295 | 6-WUR | 0.8856 | 7-WUR | 0.5945 | 9-WUR | 0.9279 | 10-WUR | 0.5840 | 11-WUR | 0.8443 |

sampling analysis while not harming the architecture itself through the sampling process.

1) Nondestructive In-situ Investigation

The nondestructive in-situ investigations are microscopic observation (Nikon Shuttle Pix P-400Rv), elemental investigation (Bruker AXS, S1TURBO portable XRF device, 45s analysis time) and colorimetric measurements (Nippon Denshoku Industries Co., Ltd, NF333, D65/10°). The detected intensities of XRF analysis for each element were applied to represent the relative element concentrations of every investigation point in this research. The results of colorimetric measurements was summarized by the 1976 CIE $L^*a^*b^*$ equation, in which L^* represents the lightness-darkness (+white, -black), a^* represents redness-greenness (+red, -green), b^* represents yellowness-blueness (+yellow, -blue). The L^* values were selected to represent degree of whitening⁵.

Through microscopic observation for whitening areas, whitish particles were observed in whitening wood, whereas some were not. Thus the type of whitening phenomenon were classified as “particle-attached” type and “no-particle-attached” type. The elemental investigation of the wooden structures of sections with copper components presented an inverse relationship between distance from copper components and Cu contents. The relationship between Cu contents and degree of whiteness were studied by calculating the correlation coefficients (r) for detected intensities of Copper (I (Cu)) and L^* value of vertical window frames (Table. 1). In some sections, such as the No. 5, No. 6 sections, the r values were close to 1, which suggest a strong positive relationship between I (Cu) and L^* values. While in some parts, such as in parts of 7-WLL ($r=0.6901$), 7-WLR ($r=0.5214$), 7-WUR ($r=0.5945$), 9-WLR ($r=0.7731$), 10-WLL ($r=0.7022$), 10-WUL ($r=0.7415$), 10-WUR ($r=0.5840$), the lower r values suggest relative weak positive relationships between I (Cu) and L^* values⁶. In brief, it was

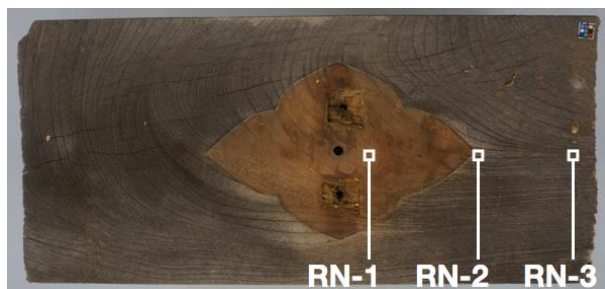


Fig. 1 Investigation points of the removed Nageshi

Table 2 Assignments of characteristic bands related to wood constituents

| Wavenumber (cm ⁻¹) | Functional Group | Assignment |
|--------------------------------------|---|--|
| 1740 | C=O stretching in unconjugated ketones aldehydes and carboxyl | Xylan Hemicellulose carboxylic acids |
| 1593 | C=C stretching of aromatic skeletal (syringyl nuclei) | Ligin |
| 1510 (soft wood) 1502 (hard wood) | C=C stretching of aromatic skeletal (guaiacyl nuclei) | Ligin |
| 1462 | C-H deformation | Ligin |
| 1423 | CH ₂ bending | Cellulose (crystallized I and amorphous) |
| 1369 | C-H deformation | Cellulose/ Hemicellulose |
| 1336 | OH in plane bending | Cellulose (amorphous) |
| 1317 | CH ₂ wagging | Cellulose (crystallised I) |
| 1268 (soft wood) | Syringyl ring C-O stretching | Ligin |
| 1236 (hard wood) | C-O stretch C-O linkage in guaiacyl aromatic methyl groups | Lignin |
| 1160 | C-O-C vibration (glucopyranose ring vibration) | Cellulose Hemicellulose |
| 1122 | Aromatic skeletal C-O stretching | Ligin |
| 1030 | C-O stretch | Cellulose Hemicellulose |
| 896 | C-H deformation C ₁ group frequency | Cellulose Hemicellulose |

confirmed that a correlation between Cu contents and degree of whiteness could not be simply concluded through a linear relationship.

2) Extra-situ Investigation

Before being removed, copper components were utilized to cover and decorate iron nails that connected pillars and Nageshi. After being exposed under the rural environment for 3 years, the parts once covered by the copper components could be easily distinguished according to clearly visible traces, which matched exactly to the Nageshi copper components, and its less degraded surface states. A significant whitening phenomenon was observed in wooden parts formerly adjacent to copper components while not in parts distanced from copper components.

To study the degradation characteristics of the different parts of in the removed Nageshi, 3 points were investigated by nondestructive methods and sampling method respectively:

1) a point of the part formerly covered by copper components (RN-1 point), 2) a point of the part formerly adjacent to copper components (RN-2 point), 3) a point of the part 6 cm distanced from copper components trace (RN-3 point) (Fig.1).

Table 3 Height ratios of absorbance bands of spectra for the RN-1, RN-2, RN-3 points

| Point | I_{1030}/I | | | | | | | | | | | |
|-------|--------------------------|-----------------|--------------------------|-----------------|--------------------------|-----------------|--------------------------|-----------------|--------------------------|-----------------|--------------------------|-----------------|
| | 1740 cm ⁻¹ | Δ (%) | 1590 cm ⁻¹ | Δ (%) | 1502 cm ⁻¹ | Δ (%) | 1462 cm ⁻¹ | Δ (%) | 1423 cm ⁻¹ | Δ (%) | 1369 cm ⁻¹ | Δ (%) |
| RN-1 | 3.87 | | 1.16 | | 1.20 | | 0.93 | | 1.13 | | 1.10 | |
| RN-2 | - | - | 3.33 | 186.9 | 2.72 | 127.5 | 19.84 | 2028.6 | 2.04 | 80.1 | 1.88 | 71.7 |
| RN-3 | 4.51 | 16.6 | 1.90 | 63.8 | 1.63 | 36.6 | 2.69 | 188.5 | 1.44 | 27.1 | 1.70 | 55.5 |

| point | I_{1030}/I | | | | | | | | | | | |
|-------|--------------------------|-----------------|--------------------------|-----------------|--------------------------|-----------------|--------------------------|-----------------|--------------------------|-----------------|-------------------------|-----------------|
| | 1336 cm ⁻¹ | Δ (%) | 1317 cm ⁻¹ | Δ (%) | 1236 cm ⁻¹ | Δ (%) | 1160 cm ⁻¹ | Δ (%) | 1122 cm ⁻¹ | Δ (%) | 896 cm ⁻¹ | Δ (%) |
| RN-1 | 4.74 | | 3.09 | | 0.61 | | 0.64 | | 1.95 | | 1.11 | |
| RN-2 | 5.29 | 11.5 | 2.57 | -17.0 | 2.60 | 325.4 | 0.70 | 9.1 | 6.29 | 222.6 | 1.78 | 59.8 |
| RN-3 | 5.43 | 14.4 | 2.52 | -18.5 | 1.72 | 181.7 | 0.70 | 9.1 | 3.33 | 70.7 | 1.48 | 33.4 |

Table 4 I_{1336}/I_{1317} , the IR-CI, the XRD-CI, and the size of crystallite for the RN-1, RN-2, RN-3 points

| Point | I_{1336}/I_{1317} | $\Delta I_{1336}/I_{1317}$ (%) | IR-CI I_{1423}/I_{896} | Δ IR-CI (%) | XRD-CI (%) | Δ XRD-CI (%) | Size of Crystallite (nm) | Δ Size (%) |
|-------|---------------------|--------------------------------|-----------------------------|--------------------|------------|---------------------|-----------------------------|-------------------|
| RN-1 | 0.65 | | 0.98 | | 36.9 | | 27.1 | |
| RN-2 | 0.49 | -25.5 | 0.87 | -11.2 | 61.1 | 65.6 | 30.6 | 12.9 |
| RN-3 | 0.46 | -28.7 | 1.03 | 5.0 | 60.0 | 62.6 | 29.1 | 7.4 |

Through nondestructive investigation for removed Nageshi, it was confirmed that whitening areas that were once adjacent to copper components contained higher Cu element, while no particle attached on the wood tissues were observed.

Extra-situ analysis included XRD analysis (Bruker AXS, D8 ADVANCE/TSM, 40mV/40mA, 0.5 sec/step), and FTIR-ATR analysis (PerkinElmer, Spectrum One(B), 4 cm⁻¹ resolution, 64 scans). Surface tissue samples were taken with a double blade razor without pretreatment.

Assignments of characteristic bands of FTIR spectra related to wood constituents were conducted on the basis of previous studies, and summarized in Table 2^{7,8}.

Chemical degradation of wood constituents (cellulose, hemicellulose, and lignin) can be reflected by FTIR spectra. In order to evaluate changes of characteristic bands related to wood constituents quantitatively, heights of characteristic bands that assigned to wood constituents of FTIR spectra were ratioed with the selected internal reference, a band at 1030 cm⁻¹. The results are shown in Table 3.

Since cellulose possesses both crystalline and amorphous region, degradation of cellulose in wood can be evaluate by crystalline portion. The height ratio of bands at 1336 cm⁻¹ and 1317 cm⁻¹ can decrease when the content of crystallized cellulose increase⁹. The height ratio of bands at 1423 cm⁻¹ and 896 cm⁻¹ can decrease, in the process of de-crystallization, which is referred as the Lateral Order Indexes, or IR Crystallinity Index (IR-CI)¹⁰. Besides, the CI

and the size of crystallite can be calculated by X-ray diffraction spectrum⁹.

The height ratio of I_{1336}/I_{1317} , the IR-CI, the XRD Crystallinity Index (XRD-CI), and the size of crystallite are presented in Table 4. The Δ shown in Table 3 is the percentage of variations of height ratios compared to the reference spectrum (RN-1).

Results of FTIR and XRD analysis suggested that in whitening areas, which contained higher Cu elements, cellulose, hemicellulose and lignin were more severely degraded, especially the latter two. The fact that acid treatments combined with accelerated thermal aging might result in a significant increase in the crystallinity index has been confirmed by some researchers¹¹. An increase of crystallinity relative to overall degradation of carbohydrate constituents implied that wood tissues of this area might have experienced complicated more degradations and transitions of cellulose.

3. Study for the Old Iwasaki-ke Suehiro-bettei Villa

The Old Iwasaki-ke Suehiro-bettei Villa is located at northwest of Tomisato City, Chiba Prefecture. It was constructed by Iwasaki Hisaya, who was the commander of Mitsubishi Zaibatsu, at the beginning of Showa period for developing the agricultural industry in Tomisato City. As a reflection of upper-class lifestyle in the beginning of the Showa period, the Main House (主屋), the Arbor (東屋), and



Fig. 2 Investigation point of the Arbor a) investigation points of exterior pillar, b) investigation points of the Itakabe

the Stone Storehouse (石蔵) were registered as Registration Tangible Cultural Properties of Japan in 2013¹².

In the Old Iwasaki-ke Suehiro-bettei Villa, the whitening phenomenon of wood adjacent to metal components is commonly observed, i.e., wood adjacent to the brass hinge of the shelf holders in Main House, the brass lamp bracket on the exterior side of the pillar and the copper nails of the exterior Itakabe (板壁, wooden wall) in the Arbor.

The nondestructive in-situ investigations included microscopic observation (Nikon ShuttlePix P-400Rv), elemental investigation (Bruker AXS, S1TURBO portable XRF device, 45s analysis time) and colorimetric measurements (Nippon Denshoku Industries Co., Ltd, NF333, D65/10°). Extra-situ analysis included SEM-EPMA (JEOL JXA-8530F, 15kV/50nA), XRD analysis (Bruker AXS, D8 ADVANCE/TSM, 40mV/40mA, 0.5 sec/step), IC analysis (Methrohm 883 Basic IC Plus, 0.700 mL/min, 10.48 MPa, 40 min per measurement), and FTIR-ATR analysis

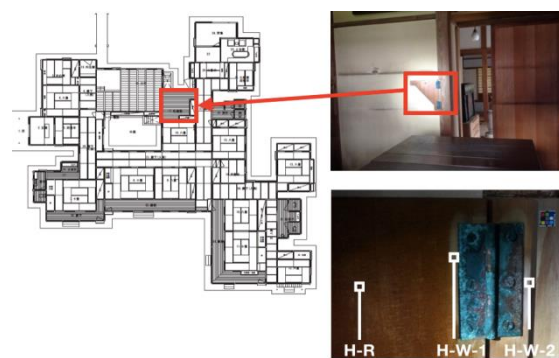


Fig. 3 Investigation points of the Main house

(PerkinElmer, Spectrum One(B), 4 cm-1 resolution, 64 scans).

Surface tissue samples were taken with a double blade razor for XRD and FTIR-ATR analyses, and taken with carbon tapes then coated with carbon for SEM-EPMA analysis. The aqueous extractives of the blade-razor-taken samples were prepared for IC analysis. Each aqueous extractive sample was prepared by immersing 0.40-0.50 mg of the original sample, which was finely powdered by agate mortar, in 5 ml ultra-pure water, incorporated with 10 min ultrasonic agitation.

The following points of the Arbor were investigated (Fig. 2, Fig. 3): a whitening point adjacent to a brass lamp bracket on the exterior side of a pillar (LB-W), a point 30 cm below the LB-W point as a normally weathered reference point (LB-Ex), a point in the interior side of the pillar as a barely weathered reference point (LB-Int), a whitening point adjacent to copper nail of the exterior Itakabe (CN-W), and a point 10 cm below CN-W point as a normally weathered reference point (CN-R). The pillar and the Itakebe of the Arbor are made from cedar. In the Main House, points around the brass hinge of a shelf holder in the pantry room

Table 5 The major results of in-situ investigation, XRD analysis and IC analysis for the Old Iwasaki-ke Suehiro-bettei Villa

| No. | Microscopic Observation | Colorimetric Measurement | | | XRF Analysis | | XRD Analysis | IC Peak Area ($\mu\text{S}/\text{cm}^2 \times \text{min}$) | | | |
|--------|-------------------------|--------------------------|-------|-------|--------------|----------|----------------------|--|----------|---------|---------|
| | | L* | a* | b* | I(Cu) | I(Zn) | | Formate | Chloride | Sulfate | Oxalate |
| LB-Int | No-particle | 44.74 | 9.99 | 21.64 | 2.03E+04 | 1.97E+04 | — | 0.0026 | 0.0131 | 0.0129 | 0.0101 |
| LB-Ex | No-particle | 33.75 | 6.70 | 15.52 | 2.01E+04 | 2.10E+04 | — | 0.0037 | 0.0252 | 0.0681 | 0.0118 |
| LB-W | Particle-attached | 57.27 | 3.04 | 11.55 | 3.14E+04 | 1.08E+06 | Zinc Oxalate Hydrate | 0.0023 | 0.0424 | 0.1715 | 0.1376 |
| CN-R | No-particle | 36.58 | 5.06 | 14.18 | 1.84E+04 | 1.71E+04 | Copper Sulfate | — | 0.0194 | 0.0753 | — |
| CN-W | Particle-attached | 49.48 | 4.92 | 18.85 | 5.04E+05 | 2.15E+04 | Moolooite | 0.0038 | 0.0258 | 0.1885 | 0.5390 |
| H-R | No-particle | 29.17 | 13.63 | 23.44 | 1.99E+04 | 1.94E+04 | — | — | 0.0194 | 0.0753 | — |
| H-W-1 | No-particle | 47.24 | 6.45 | 20.96 | 2.32E+04 | 2.22E+04 | Whewellite | 0.0206 | 0.0231 | 0.0327 | 0.0365 |
| H-W-2 | Particle-attached | 60.00 | 5.31 | 12.97 | 1.35E+04 | 1.11E+06 | Zinc Oxalate Hydrate | 0.0214 | 0.1539 | 0.0177 | 0.2407 |

Table 6 Height ratios of the FTIR spectra for investigation points in the Old Iwasaki-ke Suehiro-bettei Villa

| Point | I ₁₀₃₀ /I | | 1590 cm ⁻¹ | Δ (%) | 1510 cm ⁻¹ | Δ (%) | 1462 cm ⁻¹ | Δ (%) | 1423 cm ⁻¹ | Δ (%) |
|--------------------|--------------------------|-----------------|--------------------------|-----------------|--------------------------|-----------------|--------------------------|-----------------|--------------------------|-----------------|
| | 1740 cm ⁻¹ | Δ (%) | | | | | | | | |
| LB-Int (reference) | 10.96 | | 2.31 | | 0.96 | | 3.91 | | 1.91 | |
| LB-Ex | 10.57 | -3.6% | 2.84 | 23.2% | 1.54 | 60.5% | 6.33 | 61.9% | 2.40 | 25.6% |
| LB-W | 25.25 | 130.5% | 4.81 | 108.2% | 1.24 | 28.9% | 6.16 | 57.7% | 2.09 | 9.2% |
| CN-R | 8.27 | -24.6% | 7.82 | 238.9% | 1.22 | 27.1% | 4.27 | 9.4% | 2.82 | 47.7% |
| CN-W | 12.54 | 14.5% | 6.33 | 174.4% | 1.08 | 12.7% | 3.89 | -9.0% | 2.50 | 30.7% |
| H-R (reference) | 8.74 | | 2.12 | | 0.98 | | 3.40 | | 1.73 | |
| H-W-1 | 34.56 | 295.3% | 32.58 | 1438.4% | 3.86 | 295.5% | 30.01 | 88.7% | 2.97 | 71.8% |
| H-W-2 | 24.20 | 176.8% | 4.12 | 94.6% | 1.02 | 4.0% | 6.36 | 46.6% | 0.96 | -44.2% |

| Point | I ₁₀₃₀ /I | | 1160 cm ⁻¹ | Δ (%) | 1122 cm ⁻¹ | Δ (%) | 896 cm ⁻¹ | Δ (%) | I ₁₄₂₃ /I ₈₉₆ | | Δ (%) |
|--------------------|--------------------------|-----------------|--------------------------|-----------------|--------------------------|-----------------|-------------------------|-----------------|-------------------------------------|--|-----------------|
| | 1268 cm ⁻¹ | Δ (%) | | | | | | | | | |
| LB-Int (reference) | 1.30 | | 1.28 | | 5.03 | | 2.11 | | 1.10 | | |
| LB-Ex | 1.48 | 13.3% | 0.95 | -25.8% | 5.46 | 8.6% | 1.57 | -25.7% | 0.65 | | -40.8% |
| LB-W | 1.47 | 13.1% | 0.90 | -29.4% | 58.55 | 1063.4% | 2.35 | 11.6% | 1.13 | | 2.1% |
| CN-R | 1.43 | 9.9% | 1.22 | -4.5% | 12.78 | 154.0% | 2.32 | 10.2% | 0.82 | | -25.4% |
| CN-W | 1.36 | 4.3% | 2.03 | 58.9% | 15.77 | 213.4% | 2.71 | 28.6% | 1.09 | | -1.6% |
| H-R (reference) | 1.42 | | 1.04 | | 15.19 | | 3.00 | | 1.74 | | |
| H-W-1 | 4.97 | 250.5% | 1.03 | -1.0% | 90.03 | 492.5% | 4.35 | 45.1% | 1.47 | | -15.5% |
| H-W-2 | 1.34 | -5.2% | 1.01 | -3.5% | 2226.00 | 14549.9% | 1.76 | -41.3% | 1.83 | | 5.2% |

were investigated: a whitening point adjacent to the active side of hinge (H-W-1), a whitening point adjacent to the fixed side of hinge (H-W-2), and a point 10 cm to left of the active hinge as a barely weathered reference point (H-R). The shelf holder was made from hinoki (cypress).

The major results of the in-situ investigation, XRD analysis, and IC analysis are summarized in Table 5.

Through microscopic observation, whitish particles were observed in some whitening wood ("particle-attached type"), whereas some were not ("no-particle-attached type"). Only particle-attached type was observed in the Arbor while both the 2 types were observed in the Main House.

XRF analysis showed the high concentration of Zn and Cu in particle-attached whitening wood adjacent to brass and copper components respectively. Detected intensity of Zn in particle-attached type whitening area was extremely stronger than no-particle-attached type. SEM-EMP analysis incorporated with XRD analysis confirmed that attached particles might be predominantly formed by zinc or copper oxalate compounds corresponded to brass and copper components respectively. Through IC analysis, the significant presence of oxalate, along with the presence of sulfate or chloride were also detected in whitening samples, especially in samples of particle-attached type.

Heights of characteristic bands that are assigned to wood constituents of FTIR spectra were ratioed with the selected internal reference (band at 1030 cm⁻¹). And Lateral Order Index (height ratio of bands at 1423 cm⁻¹ and 896 cm⁻¹) was also calculated (Table 6). The Δ shown in Table 1.2 is the percentage of variations of height ratios compared to the

reference spectra (LB-Int for samples of the Arbor, H-R for samples of the Main House samples).

Combine with the content of oxalate detected by the IC analysis in each sample, significantly varied bands of FTIR spectra for oxalate contained samples which could be figured out by comparing Δ values, might provide clues about sources of oxalate (While since intensity at 1030 cm⁻¹ of the H-W-2 point was shown a significantly decrease relative to other characteristic bands, thereby height ratios for H-W-2 shown less apparent Δ values of most bands).

Results of FTIR analysis suggested that in whitening areas, either particle-attached or no-particle-attached type, hemicellulose (bands at 1740 cm⁻¹, 1160 cm⁻¹, 1030 cm⁻¹, 896 cm⁻¹) and lignin (band at 1122 cm⁻¹, especially syringyl nuclei related band at 1593 cm⁻¹) constituents were more severely attacked than normally weathered areas. Compared with no-particle-attached type, degradation of hemicellulose was more remarkable in whitening samples with attached particles. These suggest that the formation of oxalic acids may be attributed to degradation of hemicellulose and lignin of wood.

4. Conclusion

Oxalic acid is the simplest dicarboxylic acid with 3 main properties: a source of the proton, a source of the electron, and a strong metal chelator¹³. Oxalic acid commonly exists in plants, and in biosynthesis products of many wood rot fungi^{14,15}. It was firstly obtained from fusion of carbohydrates with sodium or potassium hydroxide¹. In the field of paper making industry, it has been discovered that significant oxalic

acids can be formed in the alkaline peroxide bleaching process of mechanical pulping. It is believed that most oxalic acids are formed from galacturonic and glucuronic acids, xylans, and especially lignin. In lignin constituents, syringyl units relative to guaiacyl units form more oxalates^{16,17}.

According to this, in the case of the Old Iwasaki-ke Suehiro-bettei Villa, it is possible that oxalic acids were produced by the degradation of hemicellulose and lignin constituents in wood. Degradation of wood constituents, especially the lignin units induce a whitish discoloration of wood, namely the no-particle-attached type whitening phenomenon of wood. Oxalic acid in wood, that presents high metal content, act as a strong metal chelator. Oxalic acids combine with the metal ions in wood, which migrate from metallic components during the process of corrosion, to form metallic oxalate complexes. Precipitation of whitish metallic oxalates among wood tissues leads to the particle-attached type whitening phenomenon of wood. In wood associated with copper components, copper oxalates should be formed. In wood associated with brass components, the zinc oxalate should be formed for the preferential degradation of zinc that is caused by the lower electrochemical nobility of Zn than Cu.

Additionally, metal ions may play a vital role in production of oxalic acids. However, the study for the Confucian Temple of Kodokan showed that the relationship between Cu content and degree of whiteness was not simply linear. The investigation of removed Nageshi shown that, no trace of oxalate was detected in Cu highly concentrated wood. The analysis for no-particle-attached whitening wood in the Old Iwasaki-ke Suehiro-bettei Villa showed a presence of oxalates with insignificant Zn content. Results of IC shown that, concentration of sulfate or chloride, which may accelerate corrosion of metal, were detected concomitant with oxalate in the whitening area. Therefore, it is highly possible that the formation of oxalate in wood is affected by diverse factors acting together, besides metal ions, such as an alkaline environment.

Further studies are therefore necessary to investigate more extensive cases and affecting factors to provide more comprehensive understandings about this phenomenon, and ultimately to develop the most appropriate combination plans to deal with this phenomenon caused in cultural properties.

References

- 1) R.H. FARMER: Chemistry in the Utilization of Wood, In Pergamon Series of Monographs on Furniture and Timber, 1967
- 2) 畑野経夫: 弘道館の建築、水戸市教育委員会事務局文化振興課世界遺産推進室など、近世日本の学問・教育と水戸藩: 世界遺産暫定一覧表記載資産候補「近世の教育資産」に係る平成23年度調査・研究報告書、p. 131-150、2011
- 3) 「近世日本の教育遺産群一学ぶ心・礼節の本源一」の日本遺産認定について。
<http://www.city.mito.lg.jp/000271/000273/000294/001005/002519/nihonisanninteiintuite.html> (accessed September 27, 2015)
- 4) 平成24年度孔子庙复旧工程報告書
- 5) Johnston-Feller, Ruth: Color Science in the Examination of Museum Objects: Nondestructive Procedures, Tools for Conservation, Los Angeles, Getty Conservation Institute (CA), 2001.
- 6) Allan G. Bluman: Eighth Edition Elementary Statistics A Step by Step Approach. McGraw-Hill, 2009.
- 7) Behbood Mohebbi: Attenuated Total Reflection Infrared Spectroscopy Of White-Rot Decayed Beech Wood, International Biodeterioration & Biodegradation, Volume 55, Issue 4, p.247-251, June 2005
- 8) K. K. Pandey, A. J. Pitman: Examination of the Lignin Content in Softwood and a Hardwood Decayed by a Brown-Rot Fungus with the Acetyl Bromide Method and Fourier Transform Infrared Spectroscopy, Volume 42, Issue 10, p.2340-2346, 15 May 2004
- 9) Francesca Lionetto, et al: Monitoring Wood Degradation during Weathering by Cellulose Crystallinity, Materials, p.1910-1922, 2012
- 10) Mary L. Nelson, Robert T. O'Connor. Relation of certain infrared bands to cellulose crystallinity and crystal lattice type. Part I. spectra of lattice types I, II, III and amorphous cellulose. Volume 8, Issue 3, p.1311-1324, May/June 1964
- 11) Mark Sandy, Andrew Manning, Fabrice Bollet. Changes in the Crystallinity of Cellulose in Response to Changes in Relative Humidity and Acid Treatment. Restaurator, p.1-18, 2009
- 12) 富里市教育委員会: 旧岩崎家末廣別邸保存活用基本構想、2015
- 13) Munir E, Et La: A Physiological Role For Oxalic Acid Biosynthesis In The Wood-Rotting Basidiomycete Fomitopsis Palustris, Proc Natl Acad Sci USA, 2001 Sep 25, 98(20), p.11126-30, Epub 2001 Sep 11.
- 14) Miia Ma'kela, Et La: Production Of Organic Acids And Oxalate Decarboxylase In Lignin-Degrading White Rot Fungi, Enzyme And Microbial Technology 30, p.542-549, 2002.
- 15) C.A. Clausen, Et La. Correlation Between Oxalic Acid Production And Copper Tolerance In Wolfiporia Cocos. International Biodeterioration & Biodegradation 46, P 69-76, 2000
- 16) Matti Häärä, Et La. Formation Of Oxalic Acid In Alkaline Peroxide Treatment Of Different Wood Components. Holzforschung, 68(4), P393-400, 2014
- 17) Li Yu. Oxalate Related Scaling And Its Inhibition During Peroxide Bleaching Of Mechanical Pulps. Doctor Thesis, South China University Of Technology, China, 2001